

# Interspike interval statistics of neurons that exhibit the supercritical Hopf bifurcation

Ryosuke Hosaka<sup>†, ††</sup>, Yutaka Sakai<sup>†††</sup>, Tohru Ikeguchi<sup>†</sup>, and Shuji Yoshizawa<sup>††††</sup>

<sup>†</sup>Graduate School of Science Engineering, Saitama University,  
255 Shimo-Ohkubo, Sakura-ku, Saitama 338-8570, Japan

<sup>††</sup>Aihara Complexity modelling Project, ERATO, JST, 3-23-5-201 Shibuya-ku, Tokyo 151-0064, Japan

<sup>†††</sup>Faculty of Engineering, Tamagawa University, Tokyo 194-8610, Japan

<sup>††††</sup>Tamagawa University Research Institute, Tokyo 194-8610, Japan

## Summary

We evaluated statistical characteristics of spike trains of neurons that exhibit a supercritical Hopf bifurcation by higher order statistical coefficients, a coefficient of variation and a coefficient of skewness, and showed that the estimated statistical coefficients are different from those of neurons that exhibit a subcritical Hopf bifurcation. Then, we compared the statistical coefficients of spike trains observed from cortical neurons, and showed that the neurons that exhibit the supercritical Hopf bifurcation require temporally correlated inputs to reproduce the statistical characteristics of the cortical neurons. The results indicate that it is necessary to introduce a detailed classification of neurons based on the bifurcation types of neurons. In engineering application, artificial neural networks often show high ability to solve several real life problems, for example, the pattern recognition and the combinatorial optimization problems. Although the classification or the bifurcation structure of the neurons have not been brought into the artificial neural network, an appropriate choice of an element neuron with such concept might give much advantages to solve the engineering problems with high efficiency.

## Key words:

*Hopf bifurcation, statistical analysis, Class II neurons, interspike interval, the Hindmarsh-Rose model*

## 1. Introduction

The brain comprises  $10^{11}$  neurons. In mammalian neocortex, approximately 80 % of all neurons are regularly spiking neurons. The other neurons are intrinsically bursting neurons, chattering neurons, fast spiking neurons, low-threshold spiking neurons, and late spiking neurons [2, 4, 5]. The first four neurons are excitatory neurons, and the other two are inhibitory neurons.

Aside from the above-mentioned anatomical

classification, the neurons are classified into two subcategories by firing frequency in response to constant inputs. Figure 1 shows schematic representation of firing frequency characteristics of the two subcategories. When the injected constant input is slowly ramped up, a Class I neuron starts firing with a low frequency from a critical point of firing, then its firing frequency continuously increases. On the other hand, the firing frequency of Class II neurons jumped up at a critical frequency, then the Class II neuron starts firing at a high frequency. By this classification, the regularly spiking neuron is classified into the Class I neurons, while the fast spiking neuron is classified into the Class II neurons [18].

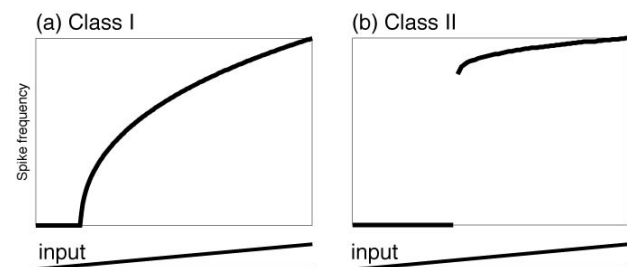


Fig. 1 Schemata of firing frequency of Class I and Class II neurons. Lower lines indicate a strength of the constant input.

In simulation studies, the neurons are often modeled by a set of differential equations, or a dynamical system. A type of excitability of the neurons is realized by a bifurcation structure of the dynamical system; a stable equilibrium changes to an unstable equilibrium surrounded by a stable limit cycle. However, the Class I and Class II neurons are realized by different bifurcations [13]. The Class I neuron can be modeled by a dynamical system exhibiting a saddle-node bifurcation, while the Class II neuron can be modeled by a dynamical system exhibiting an Andronov-Hopf bifurcation. Although such a classical

classification of neuron models have been frequently used in the field of neuroscience, we raise a very important issue: the classical classification into these two classes is not enough to reproduce statistical characteristics of biological neurons. Further, we show that we have to introduce a new classification based on a detailed bifurcation structure of the Andronov-Hopf bifurcation: the subcritical and supercritical Andronov-Hopf bifurcations (subAH and supAH). In the classical classifications, both Andronov-Hopf bifurcations exhibit the same Class II excitability in response to the constant input injection. Although responses of these two bifurcations to constant inputs are well known [6, 17], response characteristics to more neurobiologically realistic inputs remain unclear. One of the contribution of the present paper is that we reveal which bifurcation of the Class II neurons is intrinsic to reproduce real neural responses in mammalian cortices.

It is generally difficult to observe input currents for a neuron of a behaving animal. However, if we can assume that the incoming inputs are independent each other and the change of the membrane potential caused by incoming inputs is small enough relatively to a spiking threshold, total sum of the inputs can be approximated by uncorrelated fluctuations [19]. Therefore, we firstly consider the case of receiving the uncorrelated fluctuations as neurobiological realistic inputs.

In the previous study [10], we have already analyzed statistical characteristic of response of the neurons that exhibit the subAH, assuming that the external input is described by the continuous uncorrelated fluctuation. Then, we statistically analyzed interspike intervals (ISIs) by higher order statistical coefficients: a coefficient of variation (CV) and a coefficient of skewness (SK). In this paper, we firstly evaluated (CV,SK) of the supAH neuron, and compared them with that of the subAH neuron. Then, we showed that a variety of the pair (CV,SK) of the supAH neuron is smaller than that of the subAH neuron.

We also showed that (CV,SK) of the supAH neuron receiving uncorrelated inputs cannot reproduce the statistical feature of irregular spike trains of the cortical neurons of behaving animals [16], while that of the subAH neuron can. In Ref. [14], a leaky integrate-and-fire (LIF) neuron stimulated by temporally correlated inputs can reproduce the statistical feature of the spike trains of the cortical neurons [16]. Then, we investigated a possibility whether or not the supAH neuron stimulated by temporally correlated inputs can reproduce the (CV,SK)s of the cortical neurons. As a result, we discovered that temporal correlation of inputs is inevitable for the reproduction. Our final results hypothesize that a temporal scale of input of real cortical neurons might be fluctuated by time.

## 2. Methods

### 2.1 Inputs

#### 2.1.1 Uncorrelated inputs

We used the uncorrelated continuous fluctuation described by Eq. (1) as the uncorrelated inputs.

$$I(t) = \mu + \sigma \xi(t), \quad (1)$$

where  $\xi(t)$  is white Gaussian noise with zero mean and unit variance per unit time. The parameters  $\mu$  and  $\sigma$  control mean and variance of  $I(t)$ .

#### 2.1.2 Temporally correlated inputs

We used the temporally correlated continuous fluctuation expressed by Eq. (2) as the temporally correlated inputs.

$$\begin{cases} I(t) = \mu + \sigma \eta(t), \\ s \dot{\eta} = -\eta + \xi(t), \end{cases} \quad (2)$$

where  $\xi(t)$  is white Gaussian noise with zero mean and unit variance per unit time,  $s$  controls temporal correlation of inputs, and the parameters  $\mu$  and  $\sigma$  control the mean and the variance of  $I(t)$ .

### 2.2 The neuron models

#### 2.2.1 The neuron that exhibits the supercritical Andronov-Hopf bifurcation

We used the Hindmarsh-Rose (HR) model as a model of the supAH neuron [9]. The HR model consists of two-dimensional differential equations whose nullclines are cubic and quadratic functions. The HR model is described as follows:

$$\begin{cases} \dot{v} = 3v^2 - v^3 - w + I(t), \\ \tau \dot{w} = 3v(v + h) - w, \end{cases} \quad (3)$$

where  $v$  is membrane potential,  $w$  is a recovery variable,  $I(t)$  is an external input,  $\tau=10$  is a time constant of the system, and  $h$  is a parameter which decides the bifurcation type of the model.

In general, eigenvalues of a Jacobian matrix of the dynamical system is used for a discrimination of the bifurcation type. The method tells us that the HR model exhibits the saddle-node bifurcation for  $h = 0$  and the Andronov-Hopf bifurcation for  $h > 0$ . However, the

Jacobian method cannot distinguish the sub- and supercritical Hopf bifurcations. According to a criterion in Ref. [6], we confirmed that the HR model exhibits the supAH. We set  $h$  to 1 in this study.

We defined spike timings by using an internal variable  $s$ , to avoid double counting for accidental back steps: if  $s = 0$  and  $v > 1.5$ , then the neuron emits a spike and set  $s = 1$ , if  $s = 1$  and  $v < 0$ , then set  $s = 0$ .

### 2.2.2 The neuron that exhibits the subcritical Andronov-Hopf bifurcation

As a model of the subAH neuron, we used the the Bonhoffer-van der Pol (BvP) model [1, 3, 12]. The BvP model consists of two-dimensional differential equations whose nullclines are cubic and linear functions. The BvP model is described as follows:

$$\begin{cases} \dot{v} = v - v^3/3 - w + I(t), \\ \tau \dot{w} = kv - w, \end{cases} \quad (4)$$

where  $v$  is membrane potential,  $w$  is the recovery variable,  $I(t)$  is the external input, and  $\tau = 11.25$  is the temporal constant of the system. We set  $k = 1.25$ .

We defined spike timings by using an internal variable  $s$ , to avoid double counting for accidental back steps: if  $s = 0$  and  $v > 1$ , then the neuron emits a spike and set  $s = 1$ , if  $s = 1$  and  $v < 0$ , then set  $s = 0$ .

### 2.3 Statistical coefficients for ISI trains

We used two statistical coefficients, CV and SK, to statistically analyze the spike trains.

$$CV = \sqrt{(T_i - \bar{T})^2 / \bar{T}}, \quad (5)$$

$$SK = \frac{(T_i - \bar{T})^3}{\sqrt{(T_i - \bar{T})^2}}, \quad (6)$$

where  $T_i$  is the  $i$ -th ISI, determined by the series of spike timings  $\{\dots, t_i, t_{i+1}, \dots\}$  as  $T_i \equiv t_{i+1} - t_i$ ,  $\bar{T}$  represents an averaging operation over the number of ISIs, such that  $\bar{T} \equiv 1/n \sum_{i=1}^n T_i$ . CV measures a variation of the spike trains. As the variation increases, CV increases. SK measures an asymmetry in an ISI distribution. An exceptionally long ISI increases the value of SK. Regardless of the firing rate, spike event series of a Poisson process always gives  $(CV, SK) = (1, 2)$ . Conversely, the spike event series of a constant interval gives  $(CV, SK) = (0, 0)$ .

Because the above-mentioned coefficients are dimensionless quantities, we can directly compare  $(CV, SK)$  between different neurons. By contrast, we cannot compare the mean ISI or  $\bar{T}$  between the neurons.

Normalization of  $\bar{T}$  by the time scale of the neuron enables the direct comparison. The time constant of the neuron model depends on the state in the state space because of the nonlinearity of the model. However, with the parameter values used in this paper, the time constant of  $w$ ,  $\tau$ , is an upper limit on the time scale of the neuron models. We regarded  $\tau$  as the time scale of the neuron model. Hence, we compared the values of  $(CV, SK)$  between the neurons using a fixed  $\bar{T}/\tau$ . We estimated  $(\bar{T}/\tau, CV, SK)$  from finite ISI sequences consisting of 10,000 ISIs (in section 3.2) or 1,000 ISIs (in section 3.3) obtained by numerical simulations.

## 3 Results

### 3.1 Responses to constant inputs

Before we stimulate the neurons by the fluctuated inputs, let us confirm differences on amplitudes of membrane potentials of the subAH and supAH neurons receiving constant inputs. Figure 2 shows difference of the subAH and supAH in case that the strength of the constant inputs to neurons is increased or decreased.

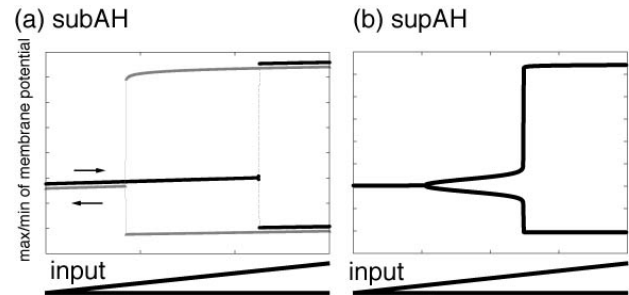


Fig. 2 Schemata of dynamic range of membrane potential of the subAH and supAH neurons receiving increasing (black lines) or decreasing (grey lines) constant inputs. Lower lines indicate a strength of the constant input. Although the real bifurcation curves are overlapped, We plot the potential with decreasing inputs (indicated by grey lines) beneath the black lines to show bistable structure.

When the strength of the constant input is increased, an equilibrium of the subAH neuron loses its stability and a large amplitude oscillation is generated (black lines in Fig.2(a)). When the strength is decreased, the large amplitude oscillation suddenly disappears and the equilibrium becomes stable again (grey lines in Fig.2(a)). However, the transition points are different by the direction of the input variation. Therefore, at the period between the two transition points, the stable equilibrium and the oscillation coexist. This bistability is sometimes called a hysteresis.

In contrast, the supAH neuron does not show the bistability. For both of increasing and decreasing inputs,

the amplitudes traces the same line. In addition, the equilibrium does not jump to the large amplitude oscillation. Instead, the supAH neuron exhibits a continuous increase from a small amplitude oscillation to the large one (Fig.2(b)).

### 3.2 Responses to the uncorrelated inputs

We calculated the statistical quantities  $(\bar{T}/\tau, CV, SK)$  as functions of the input parameters  $(\mu, \sigma)$ . These input parameters were swept, and the corresponding set of values  $(\bar{T}/\tau, CV, SK)$  were obtained. For most spiking data of cortical neurons, the condition  $\bar{T}/\tau > 1$  is satisfied. Therefore, only the spike trains that satisfy the condition were recruited as the biologically feasible spike trains.

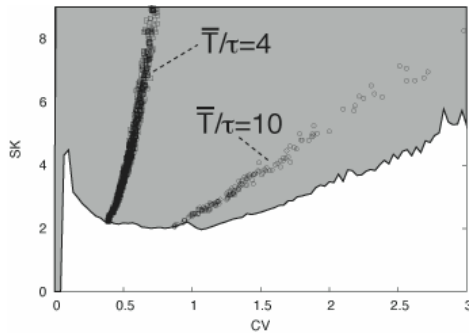


Fig. 3 Structures of the ISI statistical values  $(\bar{T}/\tau, CV, SK)$  for the subAH neuron receiving uncorrelated inputs in the CV-SK plane. The mean spike frequencies are biologically feasible (i.e.,  $\bar{T}/\tau > 1$ ) in the grey area. The open squares and open circles correspond to data for which  $\bar{T}$  is within  $\pm 1\%$  of the value satisfying  $\bar{T}/\tau = 4$  and  $10$ , respectively.

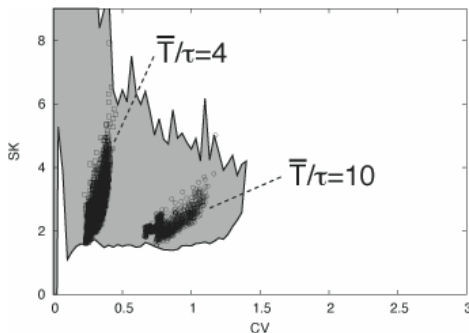


Fig. 4 The same as Fig. 3 but for the supAH neuron.

Figures 3 and 4 display the structure of the ISI statistics in the CV-SK planes for the subAH neuron [10] and the supAH neuron, respectively. As examples of the statistics, the statistics that satisfy  $\bar{T}/\tau = 4$  and  $\bar{T}/\tau = 10$  within  $\pm 1\%$  are shown in the figures. The statistics  $(CV, SK)$  for the subAH model are widely distributed on the CV-SK plane (Fig.3)[10]. We have also obtained the same characteristics for a different subAH neuron [11]. On

the other hand, in the supAH neuron, the corresponding  $(CV, SK)$  region is quite smaller than that of the supAH model (Fig.4). In particular, no spike trains that satisfy  $CV > 1.5$  were obtained.

### 3.3 Responses to the temporally correlated inputs

Experimental studies revealed that the cortical neurons of behaving animals generate irregular spike trains (see e.g., Ref.[16]). Evaluation of statistical characteristics of the cortical neurons by  $(CV, SK)$  is shown in Fig.5. The data set is obtained from neurons of a prefrontal cortex of a monkey. Each statistical coefficient is calculated from 100 ISIs (see Ref.[15] for further details of the experimental condition). As shown in Fig.5, behavior of the cortical neurons is not regular, but varies by trials. Most statistics are plotted around  $(1, 2)$  on the CV-SK plane. These spike trains have almost the same irregularity as the Poisson process. However, some spike trains show much more irregularity, because some CVs of those are larger than 2.

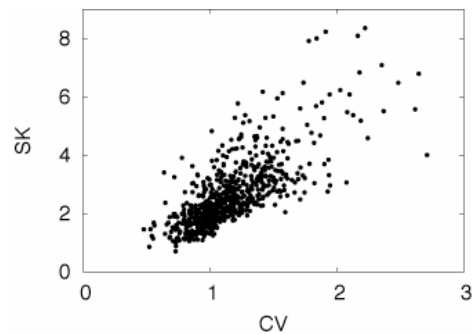


Fig. 5 An example of the statistics of cortical neurons. Each point is calculated from 100 ISIs obtained from a prefrontal cortex of a monkey.

A comparison of Figs.3 and 5 indicates that the subAH neuron stimulated by uncorrelated inputs reproduces a large variety of irregularity of the cortical neurons. On the other hand, a comparison of Figs.4 and 5 indicates that the supAH neuron stimulated by uncorrelated inputs cannot reproduce the large variety of irregularity of the cortical neurons.

It is known that the LIF neuron with the uncorrelated input cannot reproduce the large variety of irregularity of the cortical neurons [15]. The LIF neuron requires the temporally correlated inputs to reproduce the statistical characteristics of the cortical neurons [14]. In the following, we investigated whether or not the supAH neurons reproduce the statistical characteristics of the cortical neurons if inputs have temporal correlation.

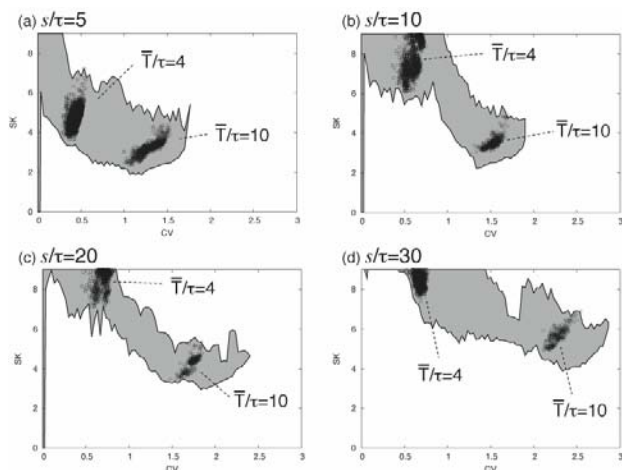


Fig.6 The same as Fig.4 but the supAH neuron receives the temporally correlated inputs.

We summarize (CV,SK) values evaluated with respect to several ratios of  $s/\tau$  in Fig.6. Assuming that  $\tau$  of the supAH neuron corresponds to 10 ms,  $s/\tau = 5$  and 10 mean that the external input has the temporal correlation of 50 and 100 ms, respectively. As shown in Fig.6, as the input correlation time scale  $s$  increases, both CV and SK increase. In the case of  $s/\tau < 10$ , the supAH neuron cannot reproduce CV that is larger than 2. If  $s/\tau$  becomes larger than 20, the supAH neurons produce CV that is larger than 2, however, (CV,SK) around (1,2) disappear, which means that the statistical coefficients of the supAH neuron do not cover the distribution of those the cortical neurons [15]. In summary, as the temporal scale of correlated inputs increases, CV and SK become large.

Above results would lead us to an interesting hypothesis: if the temporal scale of the correlated inputs to a neuron depends on time, or the correlated inputs to the neuron are nonstationary, the statistical coefficients of the supAH neuron can be a reproduction of those of the cortical neurons, because a superposition of Figs.6(a), (b), (c), and (d) shows a wide variety in the CV-SK plane. Namely, the temporal scale of the input correlation must fluctuate trial by trial to reproduce the statistical coefficients of the cortical neurons with the supAH neurons. The fluctuation of input correlation might come from conditions of the neural network.

#### 4 Discussions

In conventional studies of neuroscience, the classification of neurons is mainly discussed from the difference of the firing frequency in response to constant inputs, and the precise bifurcation structure has not been considered. Our results strongly suggest that it is inevitable to consider the precise bifurcation structure of the neuron in order to

correctly classify the neuron receiving fluctuated inputs. Based on this conjecture, we have to introduce at least three classes by its bifurcation types to classify neurons. Although the bifurcation structure of biological neurons cannot be explicitly known, the excitability, the Class I or the Class II, and the existence of the bistability implicitly tell us the bifurcation structure.

In engineering application, artificial neural networks often show high ability to solve several real life problems, for example, the pattern recognition and the combinatorial optimization problems [7, 8]. Although the classification or the bifurcation structure of the neurons have not been brought into the artificial neural network, an appropriate choice of an element neuron with such concept might give much advantages to solve the engineering problems with high efficiency.

#### Acknowledgment

The research of Y.S. was partially supported by Grant-in-Aids for Scientific Research on Priority Areas (Advanced Brain Science Project) from MEXT (No.14016002). The research of T.I. was partially supported by Grant-in-Aids for Scientific Research (C) (No.17500136) and (B) (No.163000072).

#### References

- [1] K. F. Bonh ffer. Action of passive iron as a model for the excitation of nerve. *Journal of General Physiology*, 32:69–79, 1948.
- [2] B. W. Connors and M. J. Gutnick. Intrinsic firing patterns of diverse neocortical neurons. *Trends in Neuroscience*, 13:99–104, 1990.
- [3] R. Fitzhugh. Impulses and physiological states in theoretical models of nerve membrane. *Biophysical Journal*, 1:445–466, 1961.
- [4] J. R. Gibson, M. Belerlein, and B. W. Connors. Two networks of electrically coupled inhibitory neurons in neocortex. *Nature*, 402:75–79, 1999.
- [5] C. M. Gray and C. A. McCormick. Chattering cells: superficial pyramidal neurons contributing to the generation of synchronous oscillations in the visual cortex. *Science*, 274:109–113, 1996.
- [6] J. Guckenheimer and D. Holmes. *Nonlinear Oscillations, Dynamical Systems, and Bifurcations of Vector Fields*. Springer-Verlag, New York, 1983.
- [7] M. Hasegawa, T. Ikeguchi, and K. Aihara. Combination of chaotic neurodynamics with the 2-opt algorithm to solve traveling salesman problems. *Physical Review Letters*, Vol.79, No.12, pp.2344–2347, 1997.
- [8] M. Hasegawa, T. Ikeguchi, and K. Aihara. Solving large scale traveling salesman problems by chaotic neurodynamics. *Neural Networks*, Vol.15, No.2, pp.271–283, 2002.
- [9] J. L. Hindmarsh and R. M. Rose. A model of the nerve impulse using two first-order differential equations. *Nature*, 296:162–164, 1982.

- [10] R. Hosaka, Y. Sakai, T. Ikeguchi, and S. Yoshizawa. BvP neurons exhibit a larger variety in statistics of inter-spike intervals than LIF neurons. submitted to Journal of the physical society of Japan, 2006.
- [11] R. Hosaka, Y. Sakai, T. Ikeguchi, and S. Yoshizawa. Different responses of two types of class ii neurons for fluctuated inputs. Lecture Notes in Computer Science, 3980:596–604, 2006.
- [12] J. Nagumo, A. Arimoto, and S. Yoshizawa. An active pulse transmission line simulating nerve axon. Proceedings of the Institute of Radio Engineers, 50:2061–2070, 1962.
- [13] J. Rinzel and B. B. Ermentrout. Analysis of neural excitability and oscillations. In C. Koch and I. Segev, editors, *Methods in Neuronal Modeling*. MIT Press, 1989.
- [14] Y. Sakai, S. Funahashi, and S. Shinomoto. Temporally correlated inputs to leaky integrate-and-fire models can reproduce spiking statistics of cortical neurons. *Neural Networks*, 12:1181–1190, 1999.
- [15] S. Shinomoto, Y. Sakai, and S. Funahashi. The Ornstein-Uhlenbeck process does not reproduce spiking statistics of neurons in prefrontal cortex. *Neural Computation*, 11:935–951, 1999.
- [16] W. R. Softky and C. Koch. The highly irregular firing of cortical cells is inconsistent with temporal integration of random EPSPs. *J. Neurosci.*, 13:334–350, 1993.
- [17] S. T. Strogatz. *Nonlinear Dynamics And Chaos*. Westview Press, Cambridge, 2000.
- [18] T. Tateno, A. Harsch, and H. P. C. Robinson. Threshold firing frequency-current relationships of neurons in rat somatosensory cortex: type 1 and type 2 dynamics. *Journal of neurophysiology*, 92:2283–2294, 2004.
- [19] H. C. Tuckwell. *Introduction to theoretical neurobiology*. Cambridge University Press, 1988.